The Purpose and Age of Underwater Walls in the Bay of Elaia of Western Turkey: A Multidisciplinary Approach

Martin Seeliger,[1,*] Dominik Brill,[1] Stefan Feuser,[2] Melanie Bartz,[1] Ercan Erkul,[3] Daniel Kelterbaum,[1] Andreas Vött,[4] Christina Klein,[3] Felix Pirson,[5] and Helmut Brückner[1,*]

[1]Institute of Geography, University of Cologne, Köln, (Cologne), Germany
[2]Heinrich Schliemann-Institute for Ancient Studies, University of Rostock, Rostock, Germany
[3]Institute of Geoscience, University of Kiel, Kiel, Germany
[4]Institute for Geography, Johannes Gutenberg-Universität Mainz, Mainz, Germany
[5]German Archaeological Institute, Istanbul Department, Istanbul, Turkey

Correspondence
*Corresponding authors; E-mail: martin.seeliger@uni-koeln.de; h.brueckner@uni-koeln.de

Received
23 September 2013
Accepted
21 November 2013

Scientific editing by Jamie Woodward and Gary Huckleberry

Published online in Wiley Online Library (wileyonlinelibrary.com).

doi 10.1002/gea.21471

Pergamum (modern: Bergama) was operating an important harbour used by military forces and merchants at the city of Elaia during Hellenistic and Roman Imperial times. Harbour-related facilities such as warehouses, breakwaters and wharfs document the importance of this harbour site not only for the Pergamenians. This paper focuses on the purpose and age of six submerged wall structures situated approximately 1 km south of the ancient closed harbour basin of Elaia. Geoelectric cross-sections and semi-aquatic coring near these walls failed to detect any solid basement under the walls which excludes their possible use as breakwaters or wharfs. Instead, the walls were most likely delineating and separating evaporation ponds of salt works, which compares well with similar structures from other periods and places around the Mediterranean. Combined OSL and ^{14}C-dating determined the construction age of the installation between the 4th and 6th centuries A.D. Subsequent (re-)uses are likely and are in agreement with findings from archaeological surveys.

INTRODUCTION

Several Mediterranean harbour cities have been studied over the last years dealing with regard to landscape history, utilisation of harbour basins in general, as well as harbour-related facilities such as breakwaters and wharfs (e.g., Reinhardt & Raban, 1999; Brückner, 2003; Morhange et al. 2003; Galili, Zviely, & Weinstein-Evron, 2005; Brückner et al., 2006; Kraft et al., 2007; Marriner & Morhange, 2007; Vött et al., 2007; Marriner, Morhange, & Saghieh-Beydoun, 2008; Bini et al., 2009; Algan et al., 2011; Kızıldağ, Özdaş, & Uluğ, 2012; Stanley & Bernasconi, 2012; Brückner et al., 2013; Hadler et al., 2013; Özdaş & Kızıldağ, 2013; Seeliger et al., 2013). For most of human history—from the Stone Age to modern times—harbours have played important roles in terms of trade, travelling, maritime traffic and economic centres. Other than cities in the hinterland, harbour settlements have been exposed to risks from the sea, such as extreme wave events (storms, tsunamis) and sea level rise or fall. Harbours are also prone to siltation and abandonment. Any negative impact on harbours entails repercussions on inhabitants of the settlement and the hinterland (Knoblauch, 1981; Marriner & Morhange, 2007; Morhange & Marriner, 2010).

Archaeological and geoarchaeological fieldwork at Pergamum's harbour city started in 2006 (Pirson, 2007, 2008a, 2009, 2010, 2011; Brückner & Seeliger, 2009; Seeliger et al., 2011, 2012, 2013; Brückner et al., 2013). During Hellenistic times, when the Pergamenian kingdom was dominating Asia Minor, the Pergamenians were in need of a harbour for military and economic purposes due to the fact that the city was situated approx. 26 km inland. A site was found in the city of Elaia (Figure 1A), an insignificant harbour settlement during pre-Hellenistic times located on the Gulf of Elaia (modern: Gulf of Çandarlı) (Hansen, 1971; Radt, 1999; Cartledge, 2004; Pirson, 2004, 2008b, 2012; Zimmermann, 2011).

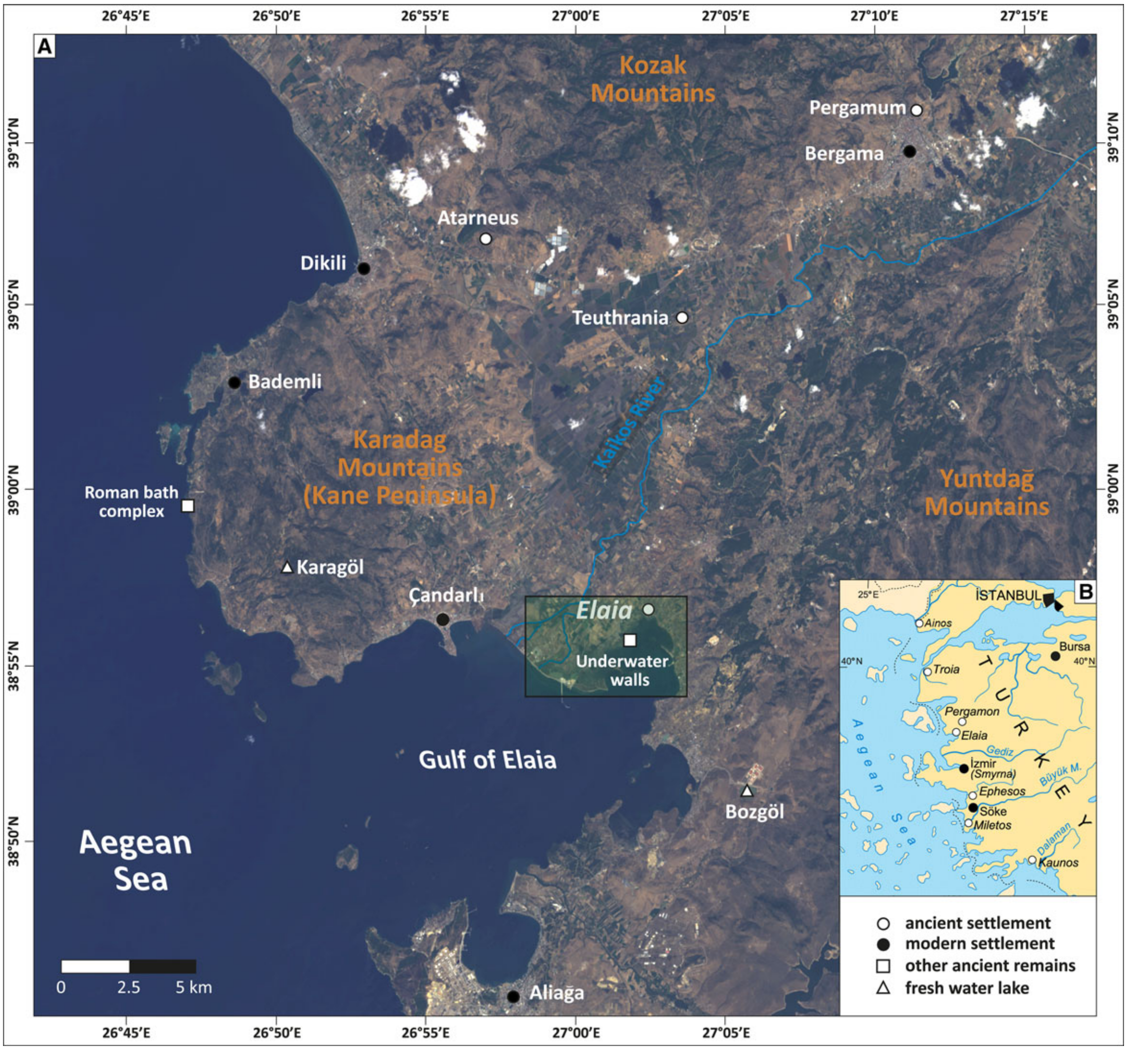

Figure 1 Area of research at the Aegean coast of Turkey. (A) Overview based on Landsat 8 (acquired September 23, 2013; composition based on bands 4, 3, 1) with locations mentioned in the text; (B) General map of western Turkey with a selection of ancient and modern settlements.

While most archaeological structures of Elaia's harbour have already been described and dated (Pirson, 2007, 2008a; Brückner & Seeliger, 2009; Seeliger, Bartz, & Brückner, 2012; Seeliger et al. 2013; Brückner et al., 2013) the purpose and age of several underwater wall structures in shallow marine waters about 1 km to the south of the closed harbour basin of Elaia remained unknown (Figure 2). In addition to the harbour breakwaters and parts of the city wall (Figure 2A), the underwater walls are the only preserved and visible remains of ancient Elaia. It has been speculated that they represent additional harbour infrastructures or shipyards far out in the embayment, breakwaters along the coast, or the remains of drowned salt works. Their age is difficult to determine because the underwater walls' blocks represent re-used building material that makes dating by archaeological criteria impossible (Pirson, 2010).

This paper presents the results of geoarchaeological, geophysical and geochronological research on six underwater wall structures in order to (i) provide a chronological framework based on luminescence and radiocarbon dating constraining their construction time and (ii) to decipher their former purpose.

AREA OF INVESTIGATION

Physical Setting

The Gulf of Elaia is situated between the Karadağ Mountains (Kane Peninsula) to the west and the Yuntdağ

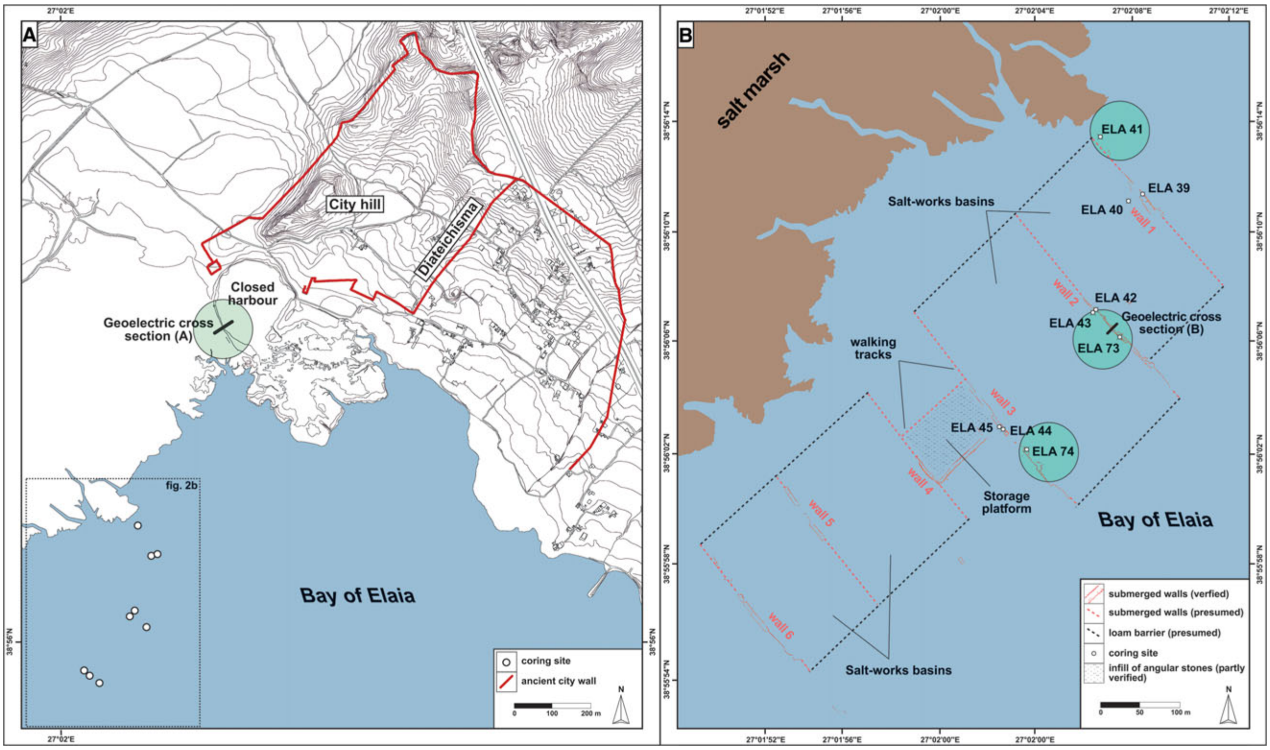

Figure 2 Location of vibracores carried out in the surroundings of the underwater walls in the Bay of Elaia. The maps are based on DGPS data levelled by the Pergamum excavation team. (A) Synoptic view with the area of the city of Elaia; (B) Location of underwater structures with associated sediment cores and geoelectric cross-sections.

mountain complex to the east (Figure 1A). It represents an area of low energy marine wave climate, even during extreme weather events during the winter season, due to its distance from the open Aegean Sea. The topography of the coastal plain as well as the bathymetry of the Bay of Elaia are relatively flat; the 20 m isobath lies ca. 4 km offshore (Aksu et al., 1987). The estimated tidal range of 20 cm determined by our DGPS (Differential Global Positioning System) surveys (Leica GPS System 530) in 2010 and 2011 are comparable to other sites in the eastern Aegean region, although wind surges may increase the sea level during the winter season (Flemming, 1978; Anzidei et al., 2011; Seeliger, Bartz, & Brückner, 2012; Seeliger et al., 2013). The modern Bakır Çay (translated: Copper River; ancient: Kaikos) forms a cuspate delta between the Kane Peninsula and the Bay of Elaia before entering the Aegean Sea (Figure 1A).

The Bay of Elaia is located on the westwards drifting Aegean–Anatolian microplate. An ensemble of several E-W-oriented late Miocene rift structures (e.g., Bergama and Zeytindağ grabens) serves as a drainage channel for the Bakır Çay, which filled the Bergama Graben with sediments (Vita-Finzi, 1969; Brinkmann, 1976; Aksu et al., 1987; McHugh et al., 2006; Schneider et al., 2011). Several archaeological sites bear witness to ongoing subsidence of the graben system, namely (i) a partly drowned Roman thermal bath situated on the western Kane Peninsula (Figure 1A) and (ii) the sunken harbour breakwaters and drowned underwater wall structures in the Bay of Elaia (Figure 1A; Seeliger, Bartz, & Brückner, 2012; Seeliger et al., 2013). Our investigations of the transgressive contact in the closed harbour area of Elaia and the study of archaeological sea level markers resulted in an estimated subsidence rate of the graben ensemble of far less than 1 m per 1000 years (Seeliger et al., 2013, in contrast to Aksu et al., 1987).

Historical Background

Pergamum is one of the most prominent ancient settlements in western Turkey mentioned in connection with Troy or Miletus (Figure 1B; Brückner et al., 2013). The city is known for the Pergamum Altar (exhibited on the Museumsinsel in Berlin, Germany) and Aelius Galenus, a famous physician in the 2nd century A.D. (Radt, 1999). As a result of the so-called Wars of the Diadochi after the death of Alexander the Great in 323 B.C., the House of the Attalids came to power in the Kaikos

Figure 3 Combined investigations at the underwater structures with geophysical measurements and coring. (A) Overview facing north; (B) Zoomed view of the wall structures (length of scale: 1 m); (C) Boat-based geoelectric measurements was done with a floating electrode cable and the RESECS instrument of the company GEOSERVE; (D) Recovering a sediment core in the shallow marine waters by using a wooden table construction. The two persons beside the zodiac are standing in the surroundings of the underwater walls.

region. The Pergamenians established their Hellenistic kingdom, which on its heyday—under king Eumenes II (197–159 B.C.)—covered most of the western part of modern Turkey. In 133 B.C. the Pergamenian kingdom was absorbed by the Roman Empire (Hansen, 1971; Radt, 1999; Cartledge, 2004; Zimmermann, 2011).

Relation Between Pergamum and Elaia

Pergamum occupies a prominent strategic location at the 330 m high city hill dominating the surrounding Kaikos plain (Figure 1A) that was optimal for defence but restricted traffic and trade. Access to the Mediterranean Sea was provided through the acquisition of nearby Elaia, situated at the Aegean Sea some 26 km southwest of Pergamum, under Eumenes I (reign: 263–241 B.C.; Pirson, 2004). Strabo mentioned Elaia as the commercial harbour of the Pergamenians and as the military base of the Attalids (Strabon: Geographica XIII, 1, 67 & XIII, 3, 5). Further literary as well as archaeological evidence underscore the close relations between Elaia and Pergamum (Pirson, 2004, 2008a, 2009, 2010).

Archaeological Setting of Underwater Wall Structures

Approx. 1 km south of the closed harbour basin (Figure 2A) six underwater wall structures trend parallel in northwest-southeast direction covering an area of ca. 1150 × 265 m^2 (Figure 2B; Pirson, 2008a). Each structure has a preserved length between 80 and 265 m and a width of 4.8 to 5.0 m (Figures 3A and B). Between the third and fourth wall a U-shaped structure has been discovered which is constructed in the same fashion. Geomagnetic measurements revealed that a similar U-shaped structure had been in place between the first and second wall (Pirson, 2010). Wave action and possible clearing of blocks may have reduced the original dimensions of the wall structures. Situated in shallow marine waters at depths of 0.5–2.0 m, the blocks rise above the silty-sandy subsoil by just a few decimetres (Figures 3A, B, and D). Well-preserved parts of walls exemplify the construction style as two parallel rows of ashlars in size of up to 0.9×0.4 m^2 in addition to quarry stones (Figures 3A and B). The space between the rows is filled up with smaller quarry stones and debris. Ashlars exhibit dowel holes on their upper sides. However, the holes of adjacent blocks are not aligned with each other and the dowels, probably originally made of bronze, are not preserved (Pirson, 2008a).

Dating of these submerged walls by archaeological or historical means has not yet been possible. The dowel holes suggest the use of recycled building material (*spolia*). The *spolia* may indicate a construction date of the walls in late Antiquity (Müller, 2003), but *spolia* usage is also known to have occurred in Roman Imperial times (Höcker, 2001). Based on archaeological or historical criteria, wall construction in Antiquity seems to be as plausible as in Byzantine or even Ottoman times.

METHODS

Geophysical and Geoarchaeological Fieldwork

Lateral and vertical changes of the archaeological and underlying sedimentary stratigraphy of the underwater wall structures were studied by interpreting sediment cores (punctual data) and geophysical measurements (cross-sections). The position and elevation of each coring site and geophysical transect was measured by using DGPS (Leica GPS System 530), with a vertical resolution of less than 2 cm. All measured altitudes are based on the gauge of Izmir and were corrected by −0.875 m to account for an inaccuracy of the PergSys05 reference system established in 2005. The resulting elevations are accurate in relation to the present sea level (Seeliger, Bartz, & Brückner, 2012, Seeliger et al., 2013).

Sediment coring was performed with an Atlas Copco Cobra pro vibracorer. A wooden platform facilitated coring in shallow marine waters (Figure 3D). Closed steel auger heads with opaque 1 m long PVC tube liners with an external diameter of 5 cm preserved cores ELA 73 and ELA 74 aphotically for OSL dating. ELA 41 was cored using open steel auger heads (diameters of 6 and 5 cm). Preliminary stratigraphies based on AG Boden (2005) were determined in the field, including characterisation of grain size, texture, roundness, colour (Munsell Soil Colour Charts), sedimentary structure, carbonate content (10 % hydrochloric acid) and macrofauna. Bulk samples of discrete sediment layers, as well as macrofossils and ceramic fragments were taken from open sediment cores for further laboratory analyses.

Earth electrical resistivity was determined with an RESECS multi-electrode system to reconstruct the thickness and shape of the closed harbour's western breakwater of Elaia (Figure 2A), and to investigate the linear underwater stone settings (electrode spacing: 1 m at the western breakwater, 2 m for cross-sections at underwater structures; Figures 2B and 3C). Several electrode arrangements were applied such as Dipole–Dipole and Wenner & Schlumberger. The apparent electrical resistivity was determined as a function of electrode geometry by the measuring instrument. Using the inversion software RESINV2D (Loke & Barker, 1995), a resistivity to depth distribution was inverted from the field data for each measured profile.

Sediment Analyses

Multi-proxy analyses were conducted in the laboratory to augment on-site facies interpretation (cf. Ernst, 1970; Vött, Handl, & Brückner, 2002, 2004; Brückner et al., 2006; Engel et al., 2009; Niwa et al., 2011; Kelterbaum et al., 2012). Samples were air-dried, ground with mortar and pestle and sieved to separate the ≤2 mm grain size fraction for further analyses. OM was decomposed via treatment with hydrogen peroxide, followed by laser-based grain size analysis with a Beckman Coulter LS13320 instrument. The calculation of grain-size parameters after Folk and Ward (1957) utilised the GRADISTAT software (Blott & Pye 2001).

Geochemical analyses included the weight LOI. Oven-dried (105°C for 12 h) samples were combusted in a furnace at 550°C for 4 h. Electric conductivity was determined in an aqueous slurry consisting of 15 g sediment in 75 mL deionised water with a glass electrode connected to a Mettler Toledo InLab®731–2m instrument. The concentrations of 30 elements were measured with a portable XRF spectrometer (Niton Xl3t 900 GOLDD; Vött et al., 2011). Sodium (Na) could not be quantified by XRF and was determined via atomic absorption spectrometry (Perkin Elmer A-Analyst 300).

Geochronological Techniques

^{14}C accelerator mass spectrometric (AMS) age determinations based on wood and charcoal were performed at the Center for Applied Isotope Studies (CAIS) of the University of Georgia, USA and at the ^{14}Chrono Centre for Climate, the Environment, and Chronology at the Queen's University Belfast, UK. All ^{14}C-dated materials

Table I Radiocarbon data set. AMS-^{14}C measurements were carried out at the Center for Applied Isotope Studies (CAIS) of the University of Georgia at Athens, USA (labcode: UGAMS) and ^{14}Chrono Centre for Climate, The Environment, and Chronology at the Queen's University Belfast, UK (labcode: UB). For calibration the Calib 7.0 software was used (Reimer et al., 2013).

Sample	Labcode	Depth (bsf)	Material	δ^{13}C (‰)	Libby-age (a)	cal A.D. (1σ)	cal A.D. (2σ)
ELA 41/5H	UGAMS 8216	1.27 m	Wood	−27.2	1780 ± 20	228–322 cal A.D.	142–332 cal A.D.
ELA 41/6H	UGAMS 8217	1.40 m	Wood	−29.5	1900 ± 25	77–126 cal A.D.	32–209 cal A.D.
ELA 41/12H	UGAMS 8219	4.50 m	Wood	−24.2	1750 ± 25	248–330 cal A.D.	232–379 cal A.D.
ELA 73/1H	UBA-22412	0.33 m	Wood	−23.4	1120 ± 37	891–974 cal A.D.	777–1013 cal A.D.
ELA 73/8H	UBA-22415	1.22 m	Charcoal	−28.5	1699 ± 29	264–391 cal A.D.	254–407 cal A.D.

bsf, below see floor.

were of terrestrial origin with relatively negative $\delta^{13}C_{VPDB}$ (‰) values (cf. Table I), wherefore a marine reservoir correction is not needed (McCormac et al., 1994). All ages were calibrated with IntCal calibration curves using Calib 7.0 software (Reimer et al., 2013) and are presented in calendar years A.D. with a 2σ range (i.e., 95.4% probability, Table I).

OSL measurements include determinations of burial doses and dose rates. The latter were estimated based on the uranium (U), thorium (Th) and potassium (K) contents in the surrounding material within a ca. 30 cm radius. U, Th and K were determined via high-resolution gamma spectrometry. The *in situ* concentrations of pore water and OM (determined by LOI) were considered for dose rate attenuation. The cosmic dose rate contribution was estimated based on geographic position, altitude above sea level, and burial depth (Prescott & Hutton, 1994). Handling and burial dose measurements of samples were performed under dimmed red light. Preprocessing included wet sieving to separate grain-size fractions of 40–63 μm, as well as chemical pre-treatment with hydrochloric acid, hydrogen peroxide and sodium oxalate to remove carbonates, OM and clay. Quartz grains were selectively preserved via etching in concentrated hexafluoro silicic acid (H_2SiF_6). Equivalent dose (D_e) measurements on a Risø TL/OSL device with a $^{90}Sr/^{90}Y$ beta radiation source, stimulation by blue LEDs (40 s) and signal detection through a Hoya U340 filter (7.5 mm) followed the SAR protocol of Murray and Wintle (2003). Small aliquots of 1 or 2 mm were measured for all samples with D_e-values between 40 and 70, using an empirically selected preheating temperature of 200°C. The calculation of burial doses was based on aliquots of samples that passed SAR acceptance criteria in terms of (i) a recycling ratio from 0.85 to 1.15, (ii) <5% recuperation of D_e, (iii) a depletion ratio of 0.9 to 1.1, and (iv) a signal-to-noise ratio above 3. Depending on the degree of signal resetting, the central age model (CAM) or the minimum age model (MAM) of Galbraith et al. (1999) were applied, using empirical σ_b-values for young coastal sediments of 15% in case of MAM (e.g., Arnold & Roberts, 2009; Brill et al., 2012). All ages were calculated with ADELE software and reflect a 1σ error (68.3%; Kulig, 2005; Table II).

RESULTS AND INTERPRETATION

Core Stratigraphies

The sedimentary context of Elaia's underwater structures was constrained by three sediment cores. Cores ELA 73 and ELA 74 were drilled directly on the archaeological structures (i.e., walls 2 and 3) between adjacent blocks, whereas core ELA 41 represents the sediment adjacent to wall 1 (Figure 2B).

Table II Luminescence data. depth b.s., sampling depth below surface; W, *in situ* water content; U, uranium; Th, thorium; K, potassium; d. rate, dose rate; Ø, aliquot size; $N_{a/m}$, number of accepted/measured aliquots; OD, over-dispersion; Sk, skewness; D_e(mean), burial dose, [a] calculated with CAM, [b] calculated with MAM. The OSL measurements were carried out in the Cologne Luminescence Lab (CLL).

Location			Dosimetry					Dose						
Sample	Labcode	Depth b.s. [m]	W [%]	U [ppm]	Th [ppm]	K [%]	d. rate [Gy/ka]	Ø [mm]	$N_{(a/m)}$	OD [%]	Sk	D_e(mean) [Gy]	Age [years]	Age [B.C./A.D.]
ELA 74/1	CL-3160	0.22	63	2.6 ± 0.1	12.7 ± 0.7	2.0 ± 0.1	2.3 ± 0.1	1	34/68	32.9	1.9	3.68 ± 0.22	1575 ± 133[b]	A.D. 307–578
								2	57/68	24.5	0.6	3.97 ± 0.24	1696 ± 145[a]	
ELA 74/2	CL-3161	0.69	51	3.3 ± 0.2	13.7 ± 0.8	2.1 ± 0.1	2.7 ± 0.1	1	34/42	13.5	0.1	6.60 ± 0.18	2406 ± 164[a]	558–230 B.C.
ELA 73/1	CL-3156	0.43	45	4.4 ± 0.2	13.6 ± 0.8	2.1 ± 0.1	3.0 ± 0.3	2	33/44	30.9	0.4	5.81 ± 0.47	1944 ± 220[b]	147 B.C.–A.D. 283
ELA 73/2	CL-3157	0.82	41	3.7 ± 0.2	14.7 ± 0.9	2.2 ± 0.1	3.1 ± 0.3	2	41/56	24.6	1.2	6.19 ± 0.63	1984 ± 240[b]	213 B.C.–A.D. 270
ELA 73/3	CL-3158	1.42	51	3.0 ± 0.2	14.3 ± 0.9	2.2 ± 0.1	2.7 ± 0.2	1	43/72	36.6	1.2	4.79 ± 0.23	1770 ± 140[b]	363 B.C.–A.D. 77
								2	37/48	21.7	1.4	4.63 ± 0.08	1712 ± 111[b]	

Sediment Core ELA 41

Core ELA 41 (Figures 2B and 4B) was drilled adjacent to the northernmost edge of the first underwater wall (27°02′19.04″ E, 38°56′35.34″ N, 0.60 m below present mean sea level, bsl) and reached a depth of 5.00 m below sea floor (bsf).

Homogeneous dark grey sand between 5.00 and 1.60 m bsf form unit 1a, with loamy silt being intercalated from 4.75 to 4.66 m bsf (Figure 4A). The Fe/Na and Na/K elemental ratios as well as LOI values express only minor fluctuations, while the electric conductivity tends to decrease upwards from 15.36 mS/cm at 4.57 m bsf to 5.87 mS/cm at 1.85 m bsf. Fragments of seagrass (*Posidonia oceanica*), wood and charcoal were encountered throughout the section. Dark greenish grey clayey silts represent unit 1b above 1.60 m bsf, with the exception of intercalating brown silty clay at 1.12 to 0.49 m bsf. (unit 2). This special clayey layer is missing in all other sediment cores described in this paper. In spite of the finer grain size at more shallow depth, the electric conductivity drops to a minimum value of 3.91 mS/cm. In addition, the sodium concentration decreases to negligible values resulting in low Na/K and high Fe/Na ratios. The finding of terrestrial plant remains, oxidation spots and lime precipitations hint to a palaeosol formation under subaerial conditions.

The cumulative sedimentological, geochemical and geophysical evidence from core ELA 41 infers deposition in a shallow marine environment for units 1a and 1b, which were interrupted temporarily by semi-terrestrial deposition (unit 2) when dry conditions exposed the accumulating sediment to terrestrial weathering and oxidation.

Sediment Core ELA 73

In contrast to ELA 41, sediment core ELA 73 (Figures 2B and 4B) was drilled through the central debris of underwater wall 2 (27°02′08.49″ E, 38°56′06.81″ N, 0.95 m bsl) reaching a depth of 2 m bsf. The basal section between 2.00 m and 1.73 m bsf is homogeneous grey sand (unit 1a) that is coarser (mean grain size 386 μm), better sorted (2.60) and has lower values of LOI (2.16%) and electric conductivity (3.95 mS/cm) compared to the rest of the profile. Silty sand between 1.75 and 1.80 m bsf indicates a depositional environment with temporarily reduced wave energy.

The section between 1.73 m and 0.51 m bsf consists of grey loamy silt with uniform geochemical and grain size characteristics that are comparable to those of the underlying stratum. Seagrass (*P. oceanica*) and mostly fragmented marine gastropods occur sporadically. From 0.51 to 0.16 m bsf the silty sediment includes abundant angular stones (unit 3). In contrast to the underlying sediment, almost all parameters trend towards the characteristics of modern sedimentation.

The profile of core ELA 73 indicates sedimentation under shallow marine conditions during deposition of units 1a and 1b. In contrast to core ELA 41, the shallow marine deposition in core ELA 73 was not interrupted by semi-terrestrial conditions, which may be due to the greater distance of ELA 73 from the shoreline. Instead, the blocks of the underwater structure (unit 3) were placed directly into shallow water strata.

Sediment Core ELA 74

Core ELA 74 (Figures 2B and 4C) was drilled through the central debris of underwater wall 3 (27°02′03.52″ E, 38°56′02.15″ N, 0.81 m bsl) and reached a depth of 1.00 m bsf. The entire profile consists of grey loamy silt expressing upward trends of decreasing Ca/K and Ca/Fe ratios that suggest a declining marine influence. Except for a thin silty sand layer at 0.35–0.38 m bsf, the grain size data show little variation. Similar to cores ELA 41 and ELA 73, the lower part of core ELA 74 includes occasional seagrass and marine gastropods. The blocks of underwater wall 3 extend from 0.35 m bsf to the seafloor (unit 3).

The profile of core ELA 74 suggests a similar scenario of sedimentation like core ELA 73. A persistent shallow marine environment seems to have extended to the time period when the blocks of underwater wall 3 (unit 3) were placed directly into the water.

Geoelectric Cross-Sections

The vertical and horizontal extent of buried parts of the underwater structures was investigated by cross-sections of electric resistivity data that ran perpendicular to the wall structures. A similar application has been successful for reconstructing the shape and penetration depth of the breakwater in Elaia's western harbour (Seeliger et al., 2013).

Geoelectric Cross-Section of the Western Harbour's Breakwater

A 46-m-long geoelectric cross-section was measured on top of the western breakwater of the closed harbour basin (cross-section A in Figures 2A and 5A). Using this field data a resistivity to depth distribution down to a depth of approx. 5 m bsf was inverted. The boulders of the breakwater are located in the central position of the profile. The calculated electrical resistivity has a bandwidth of less than 0.1–2 Ωm. Low resistivity of ≤0.3 Ωm at the outer

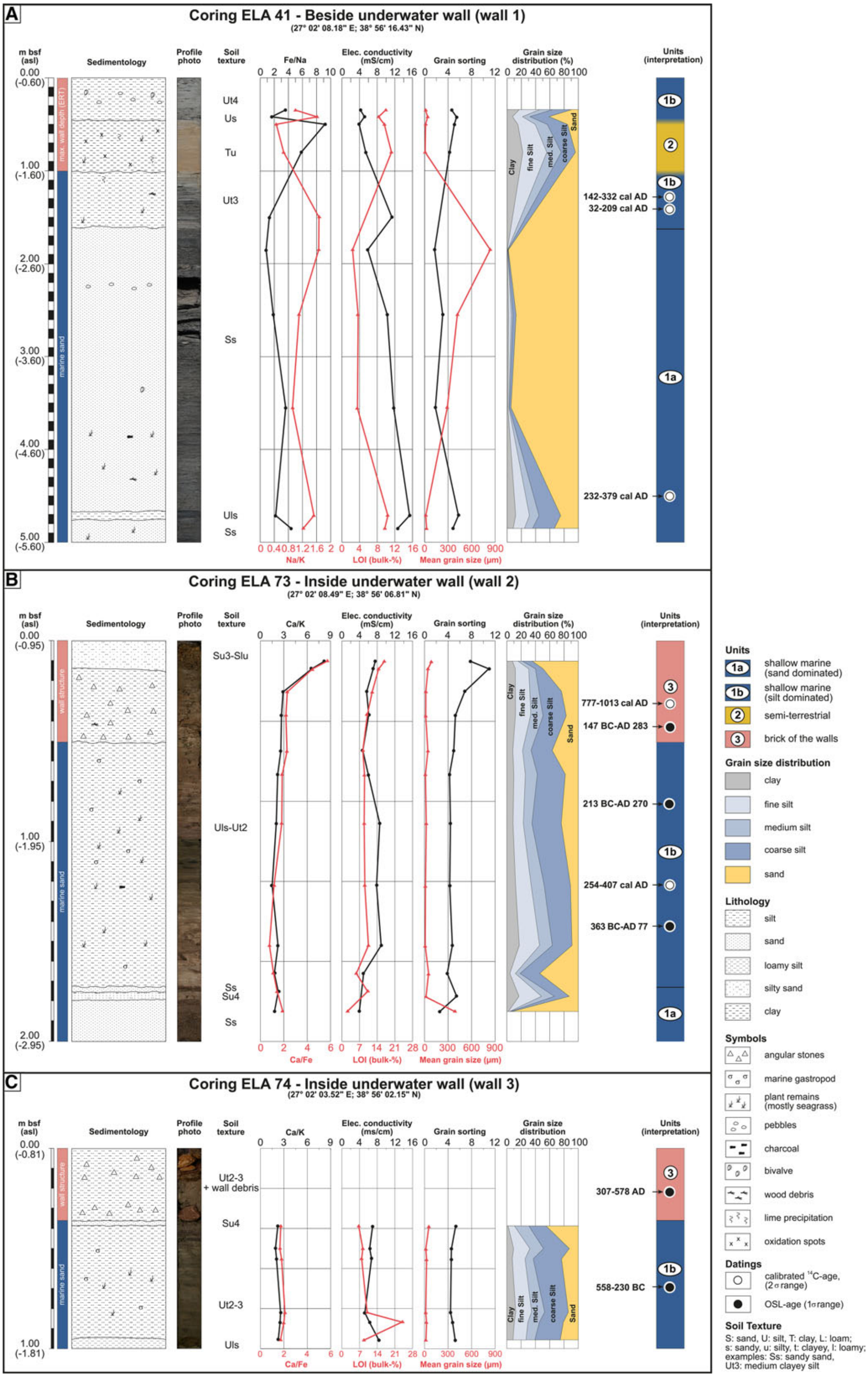

Figure 4 Stratigraphical record, facies distribution and chronological classification of cores ELA 41 (A), ELA 73 (B), and ELA 74 (C). For location of the sediment cores see Figures 2A, B.

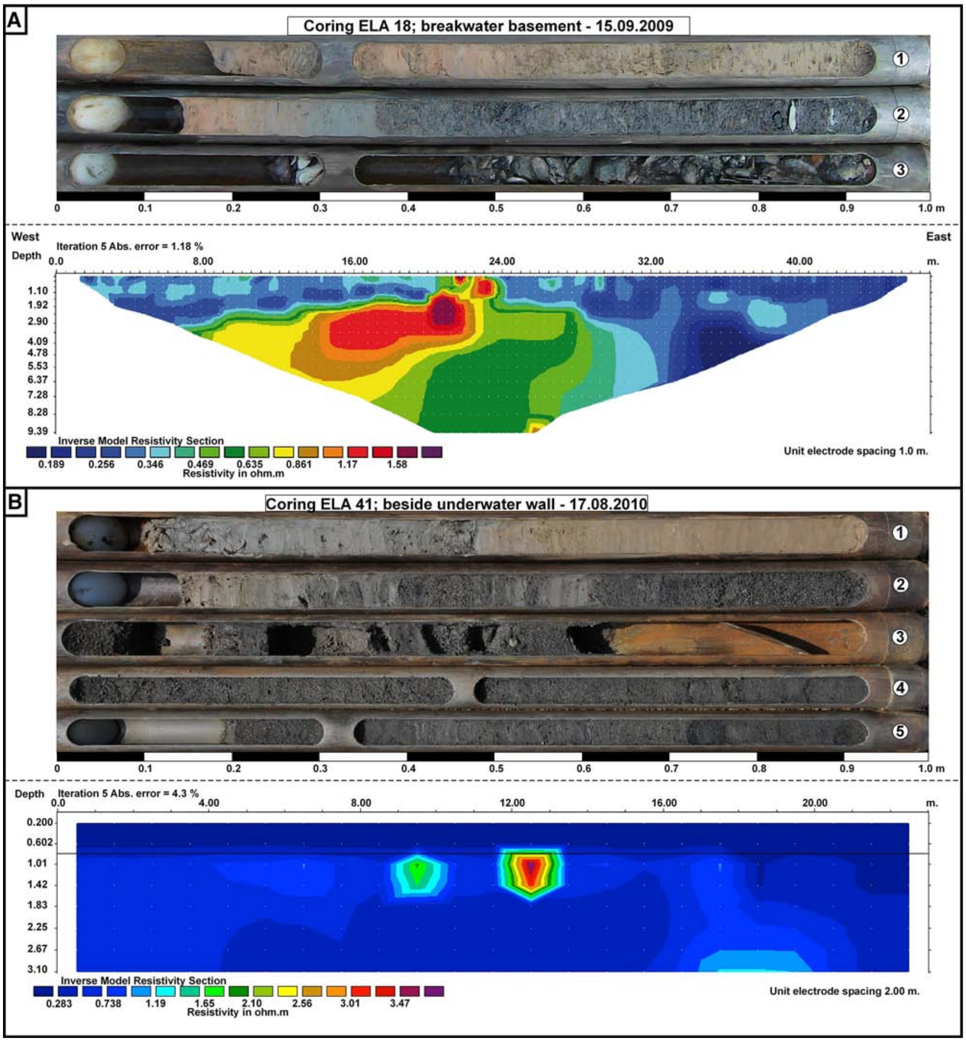

Figure 5 Earth resistivity transects for cross-sections A and B, and coring profiles of ELA 18 and 41 (for location see Figures 2A, B; Seeliger et al., 2013). The simplified inverse model section of earth resistivity measurements that were carried out by Klein and Erkul in 2010. While A shows the massive construction of the Hellenistic breakwater which even stopped the coring process at a depth of 3 m, B shows that the wall structures have no solid foundation at all; coring between two blocks only penetrated fine-grained sediments.

parts of the cross-section near the surface contrasts with highest resistivity of $\geq 2\ \Omega$m in the centre along a zone of nearly 8 m lateral and 2 m vertical extension between approx. 2 and 4 m bsf. The measured resistivity values are low compared with measurements on land because much of the electrical conductivity in marine environments is caused by dissolved salts.

Geoelectric Cross-Section of Underwater Wall 2

As a representative example for several measured profiles of underwater structures, Figure 5B illustrates a 23 m long geoelectric cross-section along the top of underwater wall 2 (cross-section B in Figure 2B). The calculated electrical resistivity reflects a bandwidth between 0.3 and 3.5 Ωm down to a depth of approx. 2 m bsf. The wall structure is located in the central position of the cross-section about 0.8 m below the present sea surface and features the highest resistivity $\geq 3.5\ \Omega$m. The electrical resistivity decreases concentrically from the centre to the periphery down to $\leq 1.6\ \Omega$m. A dislocated small boulder is discernible to the left of the centre. The width and depth of the structures stretch no more than 1 m.

Geochronology

Samples for dating were taken (i) from sediment below wall structures to establish an upper age limit of

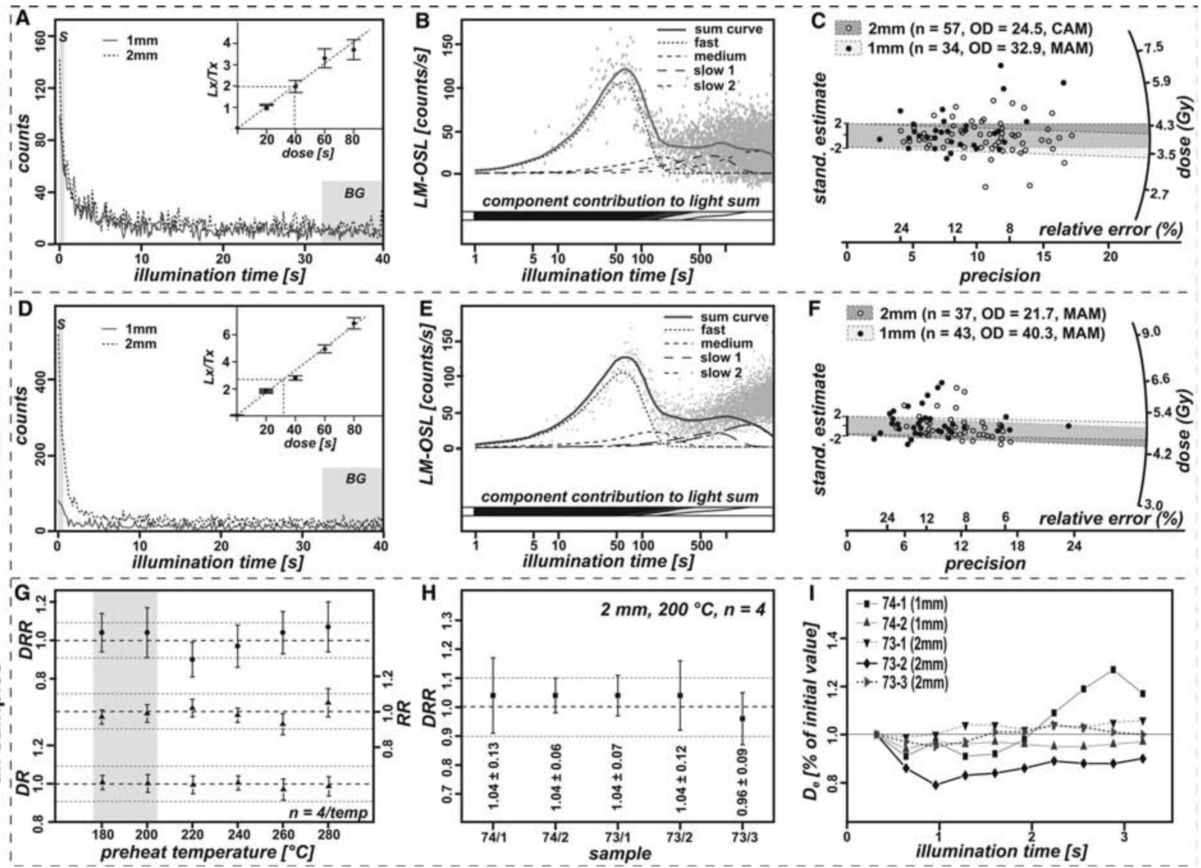

Figure 6 Luminescence properties. For cores ELA 74 and ELA 73 representative shine-down- and growth curves (A and D), LM-OSL curves (B and E) and equivalent dose distributions of 1 mm and 2 mm aliquots (C and F) are shown. While a combined dose-recovery-preheat-plateau test is shown for ELA 74/1 only (G), dose recovery tests with 200°C (H) and $D_e(t)$ plots (I) are documented for all samples. S, signal interval; BG, background interval; OD, over-dispersion; DRR, dose recovery ratio; RR, recycling ratio; DR, depletion ratio.

construction, and (ii) from within building layers to attempt a direct dating of the construction. Two marine sediment samples in unit 1 of core ELA 41, directly below the semi-terrestrial stratum (unit 2), were radiocarbon-dated (ELA 41/5H and ELA 41/6H, see Table I). Another ^{14}C date from the same core (ELA 41/12H) chronostratigraphically constrains the bottom of the profile (unit 1; Figure 4A). Core ELA 73 features two radiocarbon ages and three luminescence ages (Figure 4B). OSL sample ELA 73/1OSL and ^{14}C sample ELA 73/1H provide direct age estimates for the wall structure (unit 3), whereas OSL samples ELA 73/2OSL and ELA 73/3OSL, as well as ^{14}C sample ELA 73/8H were taken from the underlying marine unit 1. Core ELA 74 provided one luminescence sample (ELA 74/1OSL) from between the blocks of the wall (unit 3) and another one (ELA 74/2OSL) from marine sediment directly below the basement of the wall (unit 1; Figure 4C).

Luminescence Properties

Quartz grains in cores ELA 73 and ELA 74 generally show weak luminescence signals of no more than 100–500 counts (Figure 6). Although the low background of 10–30 counts still allows for D_e determination even for small 1 or 2 mm aliquots, individual measurements are afflicted by relatively large uncertainty. However, in spite of low sensitivity of quartz grains, linear modulated luminescence (LM-OSL) of samples in cores ELA 73 and ELA 74 proved the existence of a dominating fast component with a photoionisation cross-section of $\sim$1.15–1.19 $\times 10^{-17}$ cm^2 that is comparable to common empirical values (e.g., Singarayer & Bailey, 2003). More or less constant luminescence signals with increasing illumination time in $D_e(t)$ plots indicate that the fast component is thermally stable (e.g., Bailey, 2003) and may be used for equivalent dose determination.

Dose recovery tests performed on all samples yield ratios of measured dose versus laboratory dose of 0.96 ± 0.09 to 1.04 ± 0.13 ($n = 4$) and hence indicate that the applied SAR protocol for luminescence dating of quartz from both cores is appropriate. Although signal recovery was not significantly influenced by the temperature of preheating, combined tests of dose-recovery and preheating plateau revealed that performance of the SAR protocol is best for low preheating temperatures, in accordance with other studies on young marine sediments (e.g., Kiyak & Canel, 2006; Brill et al., 2012). A preheating temperature of 200°C was adopted for all routine measurements.

In case of core ELA 74, aliquots of 1 mm were favoured over 2 mm aliquots for D_e determination, since smaller aliquots are more appropriate to detect partial bleaching (Duller, 2008). Weaker signals in core ELA 73 from 1 mm aliquots with unacceptably large errors and high rejection rates prompted the use of 2 mm aliquots for D_e determination. Generally, two types of D_e distributions were observed: (i) Samples ELA 74/1OSL, 73/1OSL, 73/2OSL and 73/3OSL yielded significantly positively skewed (1.2 to 1.9) and over-dispersed (OD = 21.7 to 32.9) D_e distributions, as well as significantly higher D_e values and lower scatter for 2 mm aliquots compared to 1 mm aliquots (e.g., for ELA 74/1OSL), and point to incompletely bleached signals during deposition, prompting the use of MAM. (ii) Sample ELA 74/2OSL revealed normally distributed (skewness = 0.1) D_e values with low over-dispersion (OD = 13.5), indicating complete resetting of the luminescence signal and allowing for the use of CAM for calculating the burial dose.

Chronostratigraphy

A radiocarbon-dated fragment of wood at 4.50 m bsf in sediment core ELA 41 (Figure 4A) yielded an age of 232 to 379 cal A.D. for the base of the marine deposits (unit 1) reached in this core. Since core ELA 41 was drilled adjacent to underwater wall 1 (Figure 2B), the core lacks direct evidence of the wall structures (unit 3), such as bricks or stone fragments. However, considering the results of the geoelectric cross-section along profile B (Figure 5B), the underwater structures do not penetrate the sediment to depths of more than 1 m. Thus, the brown silty clay of unit 2 seems to be related to be related to the construction of the walls. The two ^{14}C-dated fragments of wood from the top of unit 1 at 1.27 m bsf (sample ELA 41/5H) and at 1.40 m bsf (sample ELA 41/6H), that is, immediately below unit 2, are indicating a maximum age estimate for the underwater structures. Sample ELA 41/6H yielded an age of 32 to 209 cal A.D., whereas sample ELA 41/5H dates from 142 to 332 cal A.D. (Table I).

Core ELA 73 (Figure 4B) is chronologically constrained by five ages (Tables I, II). Marine sediments of unit 1 have been dated by two luminescence samples at 1.42 m bsf (sample ELA 73/3OSL) and 0.82 m bsf (sample ELA 73/2OSL) and by a radiocarbon-dated piece of charcoal at 1.22 m bsf (sample ELA 73/8H). The three dates yield maximum ages for the underwater structure of 363 B.C. to 77 A.D., 213 B.C. to 270 A.D., and 254–407 cal A.D., respectively. Direct age information for the emplacement of the wall structures is provided by a third OSL sample at 0.43 m bsf (sample ELA 73/1OSL) with an age of 147 B.C. to 283 A.D., and by a fragment of ^{14}C-dated wood at 0.33 m bsf (sample ELA 73/1H) implying an age of 777 to 1013 cal A.D.

The underwater structure documented in sediment core ELA 74 (Figure 4C) is chronologically constrained by two luminescence ages. A first OSL sample from the marine deposits at 0.69 m bsf (unit 1b) yields a maximum limiting age of 558–230 B.C. (sample ELA 74/2OSL), and a second luminescence date (sample ELA 74/1OSL) from 0.22 m bsf (unit 2) provides a direct age of 307–578 A.D. for underwater structure 3 (Table II).

DISCUSSION

Time of Construction

Geochronological results from core ELA 41 and geoelectric profile B (Figures 2B and 5B) suggest the construction of the walls to have occurred shortly after 142–332 cal A.D. (Figure 7) during the Roman Imperial to the Late Antique period or later. The lowermost ^{14}C age of 232–379 cal A.D. (sample ELA 41/12H) is somewhat confusing. Acceptance of all three ^{14}C ages would mandate rapid sedimentation during the 3rd and 4th century A.D., which could be explained by increased sediment load of the Kaikos (Bakır Çay) due to intensified farming in its catchment area (Pirson, 2009, 2010). Unfortunately, no research concerning the late Holocene evolution of the delta has been carried out to date.

The interpretation of core ELA 74 (Figures 2B and 7) leads to similar results, indicating that the walls could have been built in the Late Antique period. According to the OSL age of sample ELA 74/1OSL, the sediment between the blocks of the walls (unit 3) was deposited between A.D. 307 and A.D. 578 (Figure 7). Thus, the erection of the walls during the Late Antique period seems to be most likely. With an age of 558–230 B.C. (sample ELA 74/2OSL), the depositional age of the shallow marine sediments immediately below the wall structure (unit 1) is in agreement with the assumed age of the

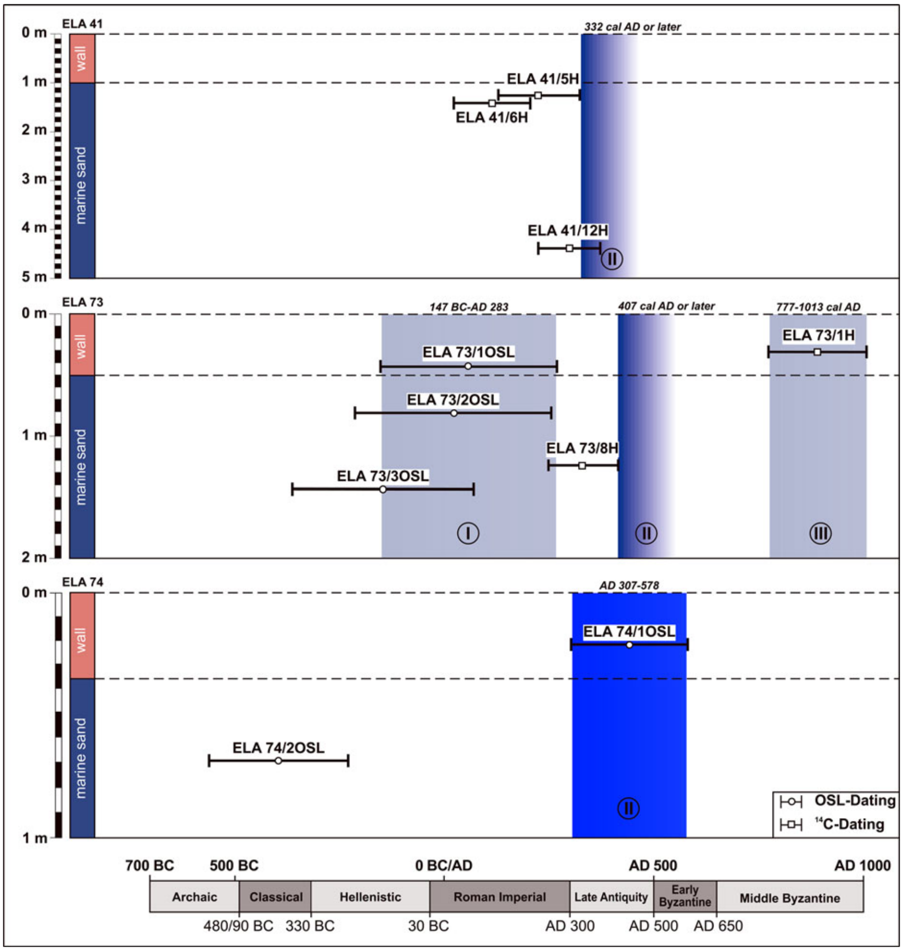

Figure 7 Synoptic chronostratigraphy of cores ELA 41, 73 and 74 (based on all measured OSL- and ^{14}C-ages) with age estimates for the time of wall construction (shaded areas). Probability II is drawn in dark blue cause it is the most likely time for the erection. Full colour shading was used for ages gained out of the wall section whereas shaded colours were used for limiting ages gained out of the marine substratum. Note that a re-use of parts of the installation is also a possible explanation for the age scatter.

structure and with results from other cores in the Bay of Elaia (Seeliger et al., 2013). Core ELA 74 features a more moderate sedimentation rate to the higher sedimentation rate of core ELA 41. It is likely that the sedimentation rate at the site of core ELA 74 was significantly less affected by the prograding Bakır Çay delta (Figures 1A and 2B).

In contrast to the similar interpretations of ages of the underwater walls based on cores ELA 41 and ELA 74, the interpretation of core ELA 73 (Figures 2B and 7) is more complicated. Although all three luminescence ages are in stratigraphically correct order, they are in conflict with the radiocarbon ages from the same profile, as well as with the chronostratigraphies of cores ELA 41 and ELA 74 (Figure 7). Three different interpretations are possible if only information from core ELA 73 is taken into account (Figure 7):

(i) If the luminescence ages are correct, the date of 147 B.C. to A.D. 283 from the lower part of unit 3 (sample ELA 73/1OSL), as well as the limiting ages of 363 B.C. to A.D. 270 from unit 1 (samples ELA 73/2OSL and ELA 73/3OSL) point to wall construction in Hellenistic to Roman Imperial times.

(ii) Acceptance of the lowermost ^{14}C age (sample ELA 73/8H) makes the wall structure younger than 254–407 cal A.D. The origin of the ^{14}C sample from nearly the same depth (1.22 m bsf) as samples ELA 41/5H (1.27 m bsf) and ELA 41/6H (1.40 m bsf) provides ages completely in agreement with the chronology of this core.

(iii) Acceptance of the uppermost ^{14}C age from within unit 3 (sample ELA 73/1H) dates the construction of wall 2 to A.D. 777–1013 A.D., that is, the Middle Byzantine times. However, this is significantly younger than postulated on the basis of cores ELA 41 and ELA 74, and relocation of the dated fragment of wood by wave action or during the coring process cannot be excluded.

Considering the fact that cores ELA 41 and ELA 74 are both pointing to a construction of the walls within the 4th to 6th centuries A.D., we consider the second interpretation to be the most likely one. The slightly older construction date of 147 B.C. to A.D. 283 proposed by the first interpretation might be influenced by inadequate assessment of partial bleaching due to insensitive samples and their weak luminescence signals. The third interpretation can be excluded if we assume relocation of the dated plant material. However, it is also possible that the wall structures 1 to 3 are not strictly contemporaneous, and that the underwater wall 2 is slightly older than structures 1 and 3. Nevertheless, the preponderance of the combined information and geochronological data of all three cores indicate a construction of the walls between the 4th and 6th centuries A.D. (Figure 7).

The Purpose of Elaia's Underwater Walls

What was the function of the underwater structures?

Most harbour infrastructures, such as shipyards or breakwaters, rely on a solid foundation to withstand heavy wave action during storms. The foundation of shipyards needs to support the weight of additional installations and ships. The closed harbour's western breakwater is an example of solidly constructed marine installations built in Hellenistic times (Figure 5A; Seeliger et al., 2013). The 8 m wide and 2 m thick foundation of the breakwater is clearly visible in geoelectric cross-section A as indicated by high values of electric resistivity (red colours in Figure 5A). The foundation is gently sloping towards the sea, whereas its harbour side shows a sharp edge with a precipitous drop to facilitate the mooring of ships (Figure 5A). The anthropogenic character of the breakwater's foundation was confirmed by sediment core ELA 18 (Figure 5A; Seeliger et al., 2013) featuring mainly rounded and angular stones, ceramics, remains of *P. oceanica* and shell debris. Based on fragments of pottery and ceramics, the structure was dated to the Hellenistic to Roman era (Seeliger et al., 2013). Massive boulders stopped the coring progress at a depth of 3 m.

In contrast to the above mentioned, the geoelectric profile B (Figure 5B) shows that Elaia's underwater wall structures are far smaller in size and are limited to approximately 1 m depth and 1 m width (Figures 2B and 5B; note the different scales of the depths axis). The lack of any extended foundation was documented by core ELA 41 (Figure 4A, 5A) and by nine sediment cores that explored the sedimentary context of the underwater structures (Figure 2B). Furthermore, the absence of dowels to fixate and link adjacent blocks indicates that the walls are lacking robust construction. We conclude that a utilisation as harbour infrastructures, shipyards, breakwaters or other solid structures can be excluded. An interpretation as *piscinae*—artificial fish ponds—is also improbable as those installations are by far smaller, of another layout and a different building technique than the wall structures in the Bay of Elaia (Higginbotham, 1997; Grüner, 2006; Evelpidou et al., 2012; Morhange et al., 2013). Plus, considering the palaeo-ecologic setting, anoxic conditions with the emission of hydrogen sulphide (H_2S) would have endangered fish farming.

Instead, similar walls have been found at several other places along the shores of the Mediterranean for compartmentalisation of evaporative ponds within marine salt works (Figure 2B). The construction design has changed little from Antiquity to modern times (Traina, 1992; Thonemann, 2011; Asencio, 2013). Additionally, the contemporaneous occurrence of semi-terrestrial conditions (unit 2 in core ELA 41; Figure 4A) in parts of the bay fits well with the assumption of salt works that would have worked only in shallow water conditions. Salt works in a shallow marine area rely on ponds that can be intermittently flooded with sea water, followed by pond closure, evaporation of sea water and harvesting of sea salt. It is known that sediments of former brines or salt pits are characterised by a higher level of calcium and magnesium compared to adjacent natural soil (Flad et al., 2005). Most probably due to leaching caused by constant water coverage over the last centuries this was not preserved in the sediments of the salt works of Elaia.

In the Bay of Elaia the former, typically rectangular wall structures of ancient salt works have mostly disappeared probably due to intentional clearing, demolition or recycling of building blocks and/or due to the weathering and destruction by wave action after the desertion of the site. Today's drowned position of the structures is incompatible which functional salt works, but can be explained by relative sea level rise or the impact of subsidence caused by eustatic, tectonic and geomorphological factors in this earthquake-prone area (Vött, 2007). At Elaia, the relative sea level has risen by approximately 1.67 m since the construction of the closed harbour's breakwater in Early Hellenistic times (Seeliger et al., 2013). Moreover, it may be assumed that the blocks have sunken into the soft substratum beneath them, especially during strong seismic events which can cause liquefaction of underlying, water-logged and unconsolidated sediment (Figure 3). Since most of the walls were demolished by human impact or partly destroyed by wave action their functional height cannot be reconstructed precisely; thus, it is impossible to use the walls as reliable sea level markers.

Does the historical background support the assumption of salt works in Elaia?

Dietary salt intake is essential for humans, especially in the warm Mediterranean climate. Salt is also needed for the well-being of livestock. Pre-modern societies frequently relied on salt for the preservation of food such as meat, cheese and fish. Literary sources of the Greek and Roman periods testify to the widespread use of salt (Blümner, 1920; Moinier, 2011). Up to the 19th century, the production of salt was limited to sea salt, mining, salt lakes and saline springs. Salt from the sea was best extracted in shallow coastal areas with hot climatic conditions. Although the climate in the Mediterranean is ideal for much of the year, there are only few favourable locations for the production of sea salt along its shorelines (Giovannini, 2000; Di Rita, Celant, & Magri, 2010). The shallow Bay of Elaia with its small tidal range of approximately 20 cm (Seeliger et al., 2013) was eminently suitable for the production of sea salt.

In the beginning of the 5th century A.D. the Roman magistrate Rutilius Namatianus describes *salinae* at Vada Volaterrana along the Etruscan coast of northern Italy (Rutilius Namatianus, De reditu suo, 470–475). Similar to the Bay of Elaia, the maritime topography of this Etruscan town is characterised by an alluvial plain deposited by two rivers. Vada Volaterrana's salt works were located near a salt marsh and represented a system of numerous canals and ponds that seems to resemble the layout of the almost contemporary salt works in the Bay of Elaia. The latter were probably built soon after the rapid aggradation of parts of the bay between the 3rd and 4th century A.D. replacing the newly evolved salt marshes. The salt works' construction was straight forward and economical with parallel rows of re-used ashlars and a fill of smaller stones in between, obviating the need for any foundation or substructure.

In Late Antiquity and Early Byzantine times of the 5th and 6th centuries the usage of the salt works in the Elaia region may have declined. In those days the population of Elaia shrank dramatically and most of the former farmland lay fallow. Elaia and its salt works were eventually abandoned and the Elaians seem to have founded a more secure settlement further inland in the area nowadays called Püsküllü Tepeler. The new settlement was separated from the sea by the foothills of the Bozyertepe, a mountain ridge that separates the Bay of Elaia from the Kaikos delta area (Pirson, 2010).

After having lain fallow for several centuries, the salt works seem to have been revived in the Late Byzantine period of the 13th century, as witnessed by a rectangular building approx. 40 m long and 20 m wide that was located on the western foothills of the Bozyertepe, at a short distance to the north-west of the Bay of Elaia (Pirson, 2009). The building is oriented towards the sea, and the approx. 1.4 km distance to the salt works could be covered easily by crossing the salt marsh (Pirson, 2009). Written sources of the 13th century describe similar salt works in the estuary region of the Büyük Menderes River near ancient Miletus that were in possession of the monastery of the island of Patmos (Thonemann, 2011).

Nothing is known from literature about the possible use of the salt works in Elaia during the subsequent Ottoman period. Production of salt in the Bay of Elaia was reported in the early 19th century by Prokesch von Osten (1837) while travelling from Pergamum to Smyrna (modern: Izmir). He observed salt works and piles of salt in the marshland area in the vicinity of the ancient city. In addition, expansive salt works are operating in the region today, for example in the coastal zone of Ayvalık north of Kaikos area (Seeliger, Bartz, & Brückner, 2012).

CONCLUSIONS

The area of the later underwater walls had been part of a shallow marine embayment when Elaia was prospering under the rule of the Pergamenians in Hellenistic and early Roman Imperial times. The water depth must have been sufficient for typical Hellenistic and later Roman ships—most maritime vessels did not require water depths in excess of 1.60 m—to reach the harbour of ancient Elaia (Coates, 1987; Beltrame & Gaddi, 2007; Marriner & Morhange, 2007; Auriemma & Solinas, 2009; Boetto, 2010; Seeliger et al., 2013). Increasing settlement activities in the hinterland seems to have caused progradation of the Bakır Çay delta and began filling the Bay of Elaia with sediment from a westerly direction since the turn of the eras. As a result, water depth decreased and a salt marsh developed (Brückner, Knipping, & Seeliger, 2010; Pirson, 2010; Seeliger, Bartz, & Brückner, 2012). Although this development was a disadvantage for shipping and trade, it offered an opportunity for the production of economically valuable sea salt.

Therefore, the underwater wall structures detected in the Bay of Elaia are best interpreted as the remains of salt works. Detailed geophysical and geoarchaeological surveys proved them to consist of blocks with a width and depth of maximally 1 m each. The walls cannot have functioned as breakwaters, piers, wharfs or any other kind of durable construction that would have needed to occasionally resist rough wave action during storms. The construction design, building technique, size and the palaeo-ecologic setting exclude a usage as fish tanks.

According to ^{14}C and OSL age estimates and in agreement with archaeological data, the walls were installed between the 4th and 6th centuries A.D. Blocks from demolished city buildings were recycled and emplaced into the salt marsh in the south-west of the bay to construct architecturally simple walls without foundation. The walls delineated and compartmentalised evaporation ponds as part of salt works. In Early Byzantine times the city of Elaia declined and was eventually abandoned, most probably because (i) the harbour's functionality became too limited, and (ii) a more secure settlement was established further inland.

Within the uncertainty of applied geochronological dating methods of this study, it is possible that not all of the wall structures have been built simultaneously. A later (re-)use and maintenance of some parts of salt works is probable as well. The eventual drowning of the walls, which makes them useless for salt works, can be attributed to eustatic sea level rise during the last ca. 1500 years, to tectonic subsidence, and to partial sinking of heavy building blocks into unconsolidated sediment when severe earthquakes may have caused sediment liquefaction.

Summing up, salt production in the region of ancient Elaia can be stated for the time soon after A.D. 300 up to the 5th or 6th centuries A.D., as well as for the 19th century A.D. The salt-works of the Late Antique period supplied Elaia, its immediate surroundings as well as the city of Pergamum with salt. There are hints given that the salt production was also in use during Late Byzantine times.

This research was conducted under the umbrella of the German Research Foundation (DFG) priority program (SPP) 1209 "The Hellenistic Polis as a Living Space – Urban Structures and Civic Identity Between Tradition and Innovation" (2008–2012). Financial support is gratefully acknowledged (DFG ref. no. PI 740/1-3). This work was part of the Elaia Survey headed by Felix Pirson, Director of the German Archaeological Institute (DAI), İstanbul Department, and excavation director in Pergamum. The investigations would not have been possible without the support and hospitality of the Pergamum excavation team. The discovery and survey of the underwater wall structures benefited from the help of Yüksel Afşin from Zeytindağ-Kazıkbağları (Turkey). Anja Zander and Nicole Klasen (both Institute of Geography, University of Cologne) helped to carry out the OSL measurements in the Cologne Luminescence Lab (CLL). Harald Stümpel (Institute of Geoscience, University of Kiel) assisted in the interpretation of geophysical data. The Geoserve company provided the electrical resistivity instrument RESECS with underwater components. The Ministry of Culture and Tourism of the Republic of Turkey kindly granted research permits. We also thank four anonymous referees for their helpful comments on an earlier version of this paper. Finally, we thank Arndt Schimmelmann (Department of Geological Sciences, Indiana University at Bloomington, USA) and Christine Seeliger (European Bioinformatics Institute, University of Cambridge, UK) for improving the manuscript language.

REFERENCES

A.G. Boden, Ed. (2005). Bodenkundliche Kartieranleitung. Stuttgart: Schweizerbart.

Algan, O., Namık Yalçın, M., Özdoğan, M., Yılmaz, Y., Sarı, E., Kırcı-Elmas, E., Yılmaz, I., Bulkan, Ö., Ongan, D., Gazioğlu, C., Nazik, A., Polat, M.A., & Meriç, E. (2011). Holocene coastal change in the ancient harbor of Yenikapı-İstanbul and its impact on cultural history. Quaternary Research, 76(1), 30–45.

Aksu, A.E., Piper, D.J.W., & Konuk, T. (1987). Late Quaternary tectonic and sedimentary history of outer İzmir and Çandarlı Bays, Western Turkey. Marine Geology, 76, 89–104.

Anzidei, M., Antonioli, F., Benini, A., Lambeck, K., Sivan, D., Serpelloni, E., & Stocchi, P. (2011). Sea level change and vertical land movements since the last two millennia along the coasts of southwestern Turkey and Israel. Quaternary International, 232, 13–20.

Arnold, L.J., & Roberts, R.G. (2009). Stochastic modelling of multi-grain equivalent dose (De) distributions: Implications for OSL dating of sediment mixtures. Quaternary Geochronology, 4, 204–230.

Asencio, A.D. (2013). Permanent salt evaporation ponds in a semi-arid Mediterranean region as model systems to study primary production processes under hypersaline conditions. Estuarine, Coastal and Shelf Science, 124, 24–33.

Auriemma, R., & Solinas, E. (2009). Archaeological remains as sea level change markers: A review. Quaternary International, 206, 134–146.

Bailey, R.M. (2003). The use of measurement-time dependent single-aliquot equivalent-dose estimates from quartz in the identification of incomplete signal resetting. Radiation Measurements, 37, 673–683.

Beltrame, C., & Gaddi, D. (2007). Preliminary analysis of the hull of the Roman ship from Grado Gorizia, Italy. International Journal of Nautical Archaeology, 36, 138–147.

Bini, M., Chelli, A., Durante, A.M., Gervasini, L., & Pappalardo, M. (2009). Geoarchaeological sea-level proxies from a silted up harbour: A case study of the Roman colony of Luni (northern Tyrrhenian Sea, Italy). Quaternary International, 206, 147–157.

Blott, S.J., & Pye, K. (2001). GRADISTAT: A grain size distribution and statistics package for the analysis of unconsolidated sediments. Earth Surface Processes and Landforms, 26, 1237–1248.

Blümner, H. (1920). s. v. Salz. In J. B. Metzler'sche (Ed.), Paulys Real-Encyclopädie der classischen Altertumswissenschaft A 1. (Sp. 2075–2099) Stuttgart: Verlagsbuchhandlung.

Boetto, G. (2010). Le port vu de la mer: l'apport de l'archéologie navale à l'étude des ports antiques. In S. Keay, G. Boetto (Eds.), Portus, Ostia and the Ports of the Roman Mediterranean. Contributions from Archaeology and History (pp. 112–128). Rome: Ministero per i Beni e le Attività Culturali.

Brill, D., Klasen, N., Brückner, H., Jankaew, K., Scheffers, A., Kelletat, D., & Scheffers, S. (2012). OSL dating of tsunami deposits from Phra Thong Island, Thailand. Quaternary Geochronology, 10, 224–229.

Brinkmann, R. (1976). Geology of Turkey. Stuttgart: Enke.

Brückner, H. (2003). Delta evolution and culture – aspects of geoarchaeological research in Miletos and Priene. In G.A. Wagner, E. Pernicka, & H.P. Uerpmann (Eds.), Troia and the Troad. Scientific approaches (pp. 121–144). Berlin, Heidelberg, New York: Springer Series: Natural Science in Archaeology.

Brückner, H., Müllenhoff, M., Gehrels, R., Herda, A., Knipping, M., & Vött, A. (2006). From archipelago to floodplain – geographical and ecological changes in Miletus and its environs during the past six millennia (Western Anatolia, Turkey). Zeitschrift für Geomorphologie N.F., Suppl. Vol. 142, 63–83.

Brückner, H., & Seeliger, M. (2009). Geoarchäologische Untersuchungen. In Pirson, F. (Ed.), Pergamon. Bericht über die Arbeiten der Kampagne 2008. Archäologischer Anzeiger, 2009(2), 194–199.

Brückner, H., Knipping, M., & Seeliger, M. (2010). Geoarchäologische Untersuchungen in der Bucht von Elaia. In Pirson, F. (Ed.), Pergamon. Bericht über die Arbeiten der Kampagne 2009. Archäologischer Anzeiger, 2010(2), 208–219.

Brückner, H., Urz, R., & Seeliger, M. (2013). Geomorphological and geoarchaeological evidence for considerable landscape changes at the coasts of western Turkey during the Holocene. Geopedology and Landscape Development Research Series, 1, 81–104.

Cartledge, P. (2004). Alexander the Great. The Hunt for a New Past. New York: Overlook Press.

Coates, J.F. (1987). Reconstructing the ancient Greek trireme warship. Endeavour, 11(2), 94–99.

Di Rita, F., Celant, A., & Magri, D. (2010). Holocene environmental instability in the wetland north of the Tiber delta (Rome, Italy): Sea-lake-man interaction. Journal of Paleolimnology, 44, 51–67.

Duller, G.A.T. (2008). Single-grain optical dating of Quaternary sediments: Why aliquot size matters in luminescence dating. Boreas, 37, 589–612.

Engel, M., Knipping, M., Brückner, H., Kiderlen, M., & Kraft, J.C. (2009). Reconstructing middle to late Holocene palaeogeographies of the lower Messenian plain (southwestern Peloponnese, Greece): Coastline migration, vegetation history and sea level change. Palaeogeography, Palaeoclimatology, Palaeoecology, 284(3–4), 257–270.

Ernst, W. (1970). Geochemical facies analysis. Amsterdam, London, New York: Elsevier.

Evelpidou, N., Pirazzoli, P., Vassilopoulos, A., Spada, G., Ruggieri, G., & Tomasin, A. (2012). Late holocene sea level reconstructions based on observations of Roman fish tanks, Tyrrhenian coast of Italy. Geoarchaeology, 27, 259–277.

Flad, R., Zhu, J., Wang, C., Chen, P, von Falkenhausen, L., Sun, Z., & Li, S. (2005). Archaeological and chemical evidence for early salt production in China. Proceedings of the National Academy of Sciences of the United States of America, 102(35), 12618–12622.

Flemming, N.C. (1978). Holocene eustatic changes and coastal tectonics in the Northeast Mediterranean: Implications for models of crustal consumption. In: Philosophical Transactions of the Royal Society of London. Mathematical and Physical Sciences, 289, 405–458.

Folk, R.L., & Ward, W.C. (1957). Brazos River bar: A study in the significance of grain size parameters. Journal of Sedimentary Petrology, 27, 3–26.

Galbraith, R.F., Roberts, R.G., Laslett, G.M., Yoshida, H., & Olley, J.M. (1999). Optical dating of single grains of quartz from Jinmium rock shelter, northern Australia. Part I: Experimental design and statistical models. Archaeometry, 41, 339–364.

Galili, E., Zviely, D., & Weinstein-Evron, M. (2005). Holocene sea level changes and landscape evolution on the northern Carmel coast (Israel). Méditerranée, 104, 79–86.

Giovannini, A. (2000). s. v. Salz. II. Griechisch-Römische Antike. In: Der Neue Pauly. Enzyklopädie der Antike 11, Verlag J. B. Metzler, Stuttgart, Sp. 1275–1278.

Grüner, A. (2006). Architektur und Ästethik römischer Fischzuchtanlagen. Zur Wahrnehmung und Funktion gattungsübergreifender Dekorationssysteme in der spätrepublikanischen Villenarchitektur, Archäologischer Anzeiger, 2006(1), 31–60.

Hadler, H., Kissas, K., Koster, B., Mathes-Schmidt, M., Mattern, T., Ntageretzis, K., Reicherter, K., Willershäuser, T., & Vött, A. (2013). Multiple late-Holocene tsunami landfall in the eastern Gulf of Corinth recorded in the palaeotsunami geo-archive at Lechaion, harbour of ancient Corinth (Peloponnese, Greece) – Zeitschrift für Geomorphologie N.F., Supplementary Issue, 4, 139–180.

Hansen, E. (1971). The Attalids of Pergamon. Ithaca: Cornell University Press.

Higginbotham, J.A. (1997). Piscinae. Artificial fishponds in Roman Italy. Chapel Hill: The University of North Carolina Press.

Höcker, Ch. (2001). s. v. Spolien. In: Der Neue Pauly. Enzyklopädie der Antike 11, Verlag J. B. Metzler, Stuttgart, Sp. 834–836.

Kelterbaum, D., Brückner, H., Dikarev, V., Gerhard, S., Pint, A., Porotov, A., & Zińko, V. (2012). Palaeogeographic changes at Lake Chokrak on the Kerch Peninsula, Ukraine, during the Mid- and Late-Holocene. Geoarchaeology, 27(3), 206–219.

Kiyak, N.G., & Canel, T. (2006). Equivalent dose in quartz from young samples using the SAR protocol and the effect of preheat temperature. Radiation Measurements, 41, 917–922.

Kızıldağ, N., Özdaş, A.H., & Uluğ, A. (2012). Late Pleistocene and Holocene Sea Level Changes in the Hisarönü Gulf, Southeast Aegean Sea. Geoarchaeology, 27, 220–236.

Knoblauch, P. (1981). Die Rolle der Strandverschiebungen bei der Rekonstruktion antiker Hafenanlagen. In J. Schäfer & W. Simon (Eds.), Strandverschiebungen in ihrer Bedeutung für Geowissenschaften und Archäologie (pp. 91–114). Heidelberg: Esprint.

Kraft, J.C., Brückner, H., Kayan, I., & Engelmann, H. (2007). The geographies of ancient Ephesus and the Artemision in Anatolia. Geoarchaeology, 22, 121–149.

Kulig, G. (2005). Erstellung einer Auswertesoftware zur Altersbestimmung mittels Lumineszenzverfahren unter spezieller Berücksichtigung des Einflusses radioaktiver Ungleichgewichte in der 238-U-Zerfallsreihe. Bachelorthesis, TU Freiberg, Freiberg.

Loke, M.H., & Barker, R.D. (1995). Least-squares deconvolution of apparent resistivity pseudosections. Geophysics, 60, 1682–1690.

Marriner, N., & Morhange, C. (2007). Geoscience of ancient Mediterranean harbours. Earth-Science Reviews, 80, 137–194.

Marriner, N., Morhange, C., & Saghieh-Beydoun, M. (2008). Geoarchaeology of Beirut's ancient harbour, Phoenicia. Journal of Archaeological Science, 35(9), 2495–2516

McCormac, F.G., Baillie, M.G.L., Pilcher, J.R., Brown, D.M., & Hoper, S.T. (1994). δ^{13}C Measurements from the Irish Oak Chronology. Radiocarbon, 36(1), 27–35.

McHugh, C.M., Seeber, L., Cormier, M., Dutton, J., Cagatay, N., Polonia, A., Ryan, W.B., & Gorur, N. 2006. Submarine earthquake geology along the North Anatolia Fault in the Marmara Sea, Turkey: A model for transform basin sedimentation. Earth and Planetary Science Letters, 248, 661–684.

Moinier, B. (2011). Salt in Antiquity: A quantification essay. In Alexianu, M., Weller, O., & Curcă, R.-G. (Eds.), Archaeology and anthropology of salt: A diachronic approach. Proceedings of the International Colloquium, 1–5 October 2008, Al. I. Cuza University (pp. 137–148). Iaşi, Romania: Oxford.

Morhange, C., Blanc, F., Bourcier, M., Carbonel, P., Prone, A., Schmitt, S., Vivent, D., & Hesnard, A. (2003). Bio-sedimentology of the late Holocene deposits of the ancient harbor of Marseilles (Southern France, Mediterranean sea). The Holocene, 13(4), 593–604.

Morhange, C., & Marriner, N. (2010). Palaeo-hazards in the coastal Mediterranean: A geoarchaeological approach. In Martini, I., & Chesworth, P.W. (Eds.), Landscapes and Societies (pp. 223–234).

Morhange, C., Marriner, N., Excoffon, P., Bonnet, S., Flaux, C., Zibrowius, H., Goiran, J.-P., & Amouri, M.E. (2013). Relative sea-level changes during Roman times in the northwest Mediterranean: The 1st century A.D. fish tank of Forum Julii, Fréjus, France. Geoarchaeology, 28, 363–372.

Müller, R. (2003). s. v. Spolien (RWG), In: Der Neue Pauly. Enzyklopädie der Antike 15/3, Verlag J. B. Metzler, Stuttgart, Sp. 195–208.

Murray, A.S., & Wintle, A.G. (2003). The single aliquot regenerative dose protocol: Potential for improvements in reliability. Radiation Measurements, 37, 377–381.

Niwa, Y., Sugai, T., Saegusa, Y., Ogami, T., & Sasao, E. (2011). Use of electrical conductivity to analyze depositional environments: Example of a Holocene delta sequence on the Nobi Plain, central Japan. Quaternary International, 230, 78–86.

Özdaş, H., & Kızıldağ, N. (2013). Archaeological and geophysical investigation of submerged coastal structures in Kekova, Southern Coast of Turkey. Geoarchaeology, 28, 504–516.

Pirson, F. (2004). Elaia, der maritime Satellit Pergamons. Istanbuler Mitteilungen, 54, 197–213.

Pirson, F. (2007). Elaia. In Pirson, F. (Ed.), Pergamon. Bericht über die Arbeiten der Kampagne 2006. Archäologischer Anzeiger, 2007(2), 47–58.

Pirson, F. (2008a). Elaia. In Pirson, F. (Ed.), Pergamon. Bericht über die Arbeiten der Kampagne 2007 (pp. 130–140). Archäologischer Anzeiger, 2008(2), 130–140.

Pirson, F. (2008b). Das Territorium der hellenistischen Residenzstadt Pergamon – Herrschaftlicher Anspruch als raumbezogene Strategie. In Jöchner, C. (Ed.), Räume der Stadt – Von der Antike bis heute (pp. 27–50). Berlin: Reimer.

Pirson, F. (2009). Elaia. In Pirson, F. (Ed.), Pergamon. Bericht über die Arbeiten der Kampagne 2008. Archäologischer Anzeiger, 2009(2), 182–200.

Pirson, F. (2010). Survey. In Pirson, F. (Ed.), Pergamon. Bericht über die Arbeiten der Kampagne 2009 (pp. 195–201). Archäologischer Anzeiger, 2010(2), 195–201.

Pirson, F. (2011). Elaia. In Pirson, F. (Ed.), Pergamon. Bericht über die Arbeiten der Kampagne 2010. Archäologischer Anzeiger, 2011(2), 166–174.

Pirson, F. (2012). Hierarchisierung des Raumes? Überlegungen zur räumlichen Organisation und deren Wahrnehmung im hellenistischen Pergamon und seinem Umland. In Pirson, F. (Ed.), Manifestationen von Macht und Hierarchien in Stadtraum und Landschaft, BYZAS, 13, 187–232. Istanbul.

Prescott, J.R., & Hutton, J.T. (1994). Cosmic ray contributions to dose rates for luminescence and ESR dating: Large depths and long-term time variations. Radiation Measurements, 23, 497–500.

Prokesch von Osten, A. (1837). Denkwürdigkeiten und Erinnerungen aus dem Orient III, Stuttgart 1837.

Radt, W. (1999). Pergamon – Geschichte und Bauten einer antiken Metropole. Darmstadt: Wissenschaftliche Buchgesellschaft.

Reimer, P.J., Bard, E., Bayliss, A., Beck, J.W., Blackwell, P.G., Bronk Ramsey, C., Buck, C.E., Cheng, H., Edwards, R.L., Friedrich, M., Grootes, P.M., Guilderson, T.P., Haflidason, H., Hajdas, I., Hatt, C., Heaton, T.J., Hogg, A.G., Hughen, K.A., Kaiser, K.F., Kromer, B., Manning, S.W., Niu, M., Reimer, R.W., Richards, D.A., Scott, E.M., Southon, J.R., Turney, C.S.M., & van der Plicht, J. (2013). IntCal13 and MARINE13 radiocarbon age calibration curves 0–50000 years calBP. Radiocarbon, 55(4), 1869–1887.

Reinhardt, E.G., & Raban, A. (1999). Destruction of Herod the Great's harbor at Caesarea Maritima, Israel – geoarchaeological evidence. Geology, 27, 811–814.

Rutilius Namatianus, De reditu suo. Translation and comments by Ernst Doblhofer I. II. Carl Winter Universitätsverlag, Heidelberg 1972 (Latin to German).

Schneider, S., Knitter, D., & Schütt, B. (2011). Geoarchäologische Untersuchungen im westlichen Kaikostal. In Pirson, F. (Ed.), Pergamon – Bericht über die Arbeiten in der Kampagne 2010. Archäologischer Anzeiger, 2011(2), 160–166.

Seeliger, M., Schneider, S., Brückner, H., Schütt, B., Horjes, B., Feuser, S., Zimmermann, M., & Pirson, F. (2011). Studying Pergamon's environs – geoarchaeological research in Elaia and Bakircay valley. Proceedings of the International Bergama Symposium, 7–9 April 2011, vol. I: 48–65. Izmir.

Seeliger, M., Bartz, M., & Brückner, H. (2012). Mauern im Meer – Geoarchäologische Untersuchungen in der Bucht von Elaia. In Pirson, F. (Ed.), Pergamon. Bericht über die Arbeiten der Kampagne 2010. Archäologischer Anzeiger, 2011(2), 175–185.

Seeliger, M., Bartz, M., Erkul, E., Feuser, S., Kelterbaum, D., Klein, C., Pirson, F., Vött, A. & Brückner, H. (2013). Taken from the sea, reclaimed by the sea: The fate of the closed harbour of Elaia, the maritime satellite city of Pergamum (Turkey). Quaternary International, 312, 70–83.

Singarayer, J.S., & Bailey, R.M. (2003). Further investigations of the quartz optically stimulated luminescence components using linear modulation. Radiation Measurements, 37, 451–458.

Stanley, J.-D., & Bernasconi, M.P. (2012). Buried and submerged Greek archaeological coastal structures and artifacts as gauges to measure late Holocene Seafloor Subsidence off Calabria, Italy. Geoarchaeology, 27, 189–205.

Strabon: Geographica. Translation and comments by Albert Forbiger. Marix Verlag, Wiesbaden 2005 (Greek to German).

Thonemann, P. (2011). The Maeander valley. A historical geography from Antiquity to Byzantium. Cambridge University Press.

Traina, G. (1992). Sale e saline nel Mediterraneo antico. La parola del passato, 47, 363–378.

Vita-Finzi, C. (1969). Late Quaternary continental deposits of central and western Turkey. Man, New Series, 4, 605–619.

Vött, A. (2007). Relative sea level changes and regional tectonic evolution of seven coastal areas in NW Greece since the mid-Holocene. Quaternary Science Reviews, 26, 894–919.

Vött, A., Handl, M., & Brückner, H. (2002). Rekonstruktion holozäner Umweltbedingungen in Akarnanien (Nordwestgriechenland) mittels Diskriminanzanalyse von geochemischen Daten. Geologica et Palaeontologica, 36, 123–147.

Vött, A., Brückner, H., Schriever, A., Handl, M., Besonen, M., & van der Borg, K. (2004). Holocene coastal evolution around the ancient seaport of Oiniadai, Acheloos alluvial plain, NW Greece. Coastline Reports, 1, 43–53.

Vött, A., Schriever, A., Handl, M., & Brückner, H. (2007). Holocene palaeogeographies of the central Acheloos River delta (NW Greece) in the vicinity of the ancient seaport Oiniadai. Geodinamica Acta, 20(4), 241–256.

Vött, A., Bareth, G., Brückner, H., Lang, F., Sakellariou, D., Hadler, H., Ntageretzis, K., & Willershäuser, T. (2011). Olympia's harbour site Pheia (Elis, Western Peloponnese, Greece) destroyed by tsunami impact. Die Erde, 142(3), 259–288.

Zimmermann, M. (2011). Pergamon: Geschichte, Kultur, Archäologie. C. H. Beck, München.

